FERMILAB-Conf-98/395-E
D0

The D0 Run II Luminosity Monitor

Chyi-Chang Miao
For the D0 Collaboration

Brown University
Providence, Rhode Island 02912

Fermi National Accelerator Laboratory
P.O. Box 500, Batavia, Illinois 60510

December 1998

Published Proceedings of the *6th International Conference on Advanced Technology and Particle Physics*, Como, Italy, October 5-9, 1998

The DØ Run II Luminosity Monitor

Chyi-Chang Miao[a]
For the DØ Collaboration[b]

[a]*Department of Physics, Box 1843, Brown University, Providence, RI 02912, U.S.A.*
E-mail: cmiao@fnal.gov

[b]*Fermilab, P.O.Box 500-MS 357, Batavia, IL, 60510-0500, U.S.A.*

The DØ Run II Luminosity Monitor consists of plastic scintillation detectors with fine-mesh photomultiplier readout that cover the range $2.7 < |\eta| < 4.4$ in pseudorapidity. The detector is designed to provide a precise measurement of the rate for non-diffractive inelastic collisions that is used to calculate the Tevatron luminosity at DØ. Excellent time-of-flight resolution allows a clean separation between beam-beam interactions and the principal background from beam halo. In addition, timing is used to measure the position of the primary interaction vertex and to detect multiple interactions. Accurate correction for multiple proton-antiproton interactions in a single beam crossing is essential for an accurate luminosity determination. Associated electronics provide a single-interaction trigger term for the DØ Level 1 trigger, and readout of the photomultiplier timing and pulse-height measurements.

1. Introduction

The primary purpose of the DØ Luminosity Monitor is to detect non-diffractive inelastic collisions with high efficiency for making an accurate determination of the Tevatron luminosity at DØ. The Luminosity Monitor counts only once for each crossing with one or more $p\bar{p}$ interactions and obtains the fraction of crossings with no interactions. Poisson statistics for the probability of zero interaction in one crossing, $P_0 = e^{-\bar{n}}$ where $\bar{n}$ is the average number of interactions per crossing, is used to determine the luminosity. This calculation therefore takes into account the multiple $p\bar{p}$ interactions that can occur within each beam crossing.

In addition, the precise time-of-flight measurement for charged particles hitting the Luminosity Monitor counters allows it to make fast determination of the vertex position, measure beam halo rates, and provide diagnostics on the beam optics at the collision point. The Luminosity Monitor also provides trigger signals to identify beam crossings with a single $p\bar{p}$ interaction, and triggers in the large η region for diffractive and rapidity gap physics at DØ.

The DØ Run I (1992-96) Luminosity Monitor [1] operation was quite successful in meeting its original design goals. The error of 5.3% in the Run I luminosity measurement [2] can be divided into two parts: a DØ related contribution (2.6%) due to uncertainties in detector acceptance and efficiency and a non-DØ contribution (4.6%) due to uncertainties in the inelastic and diffractive cross section measurement made by E710 [3] and CDF [4]. A time-of-flight resolution of 250 ps for the Run I Luminosity Monitor counters allowed determination of the vertex position to an accuracy of ~ 3.5 cm for single interaction beam crossings [1], and provided accelerator diagnostic information [5]. Also, a number of triggers in Run I with large cross sections benefited by being able to select events that predominantly had a single $p\bar{p}$ interaction. The detector further provided triggers on events with forward rapidity gaps.

The upgrade of the Fermilab accelerator complex is expected to provide the Tevatron collider program a luminosity of 2×10^{32} cm^{-2}s^{-1} and an integrated luminosity of 2 fb^{-1}. The Luminosity Monitor is one of the DØ detector upgrade projects underway to optimize the physics capabilities in Run II, maintain its excellent performance achieved in Run I, and meet the detector constraints from other components of the DØ upgrade. Two of the most significant changes seen by the Luminosity Monitor are:

- The accelerator will change the beam bunch spacing from 3.5 μs in Run I to 396 ns in the earlier stage of Run II, and later change to 132 ns bunch spacing. This requires entirely new readout electronics for the Luminosity Monitor.
- The DØ Run II detector will have a solenoid magnet providing a 2 Tesla magnetic field for its central tracking system. The conventional photomultiplier tubes used in the Run I Luminosity Monitor counters need to be replaced with a new readout technology.

In the next section, we will describe the new counter design. Results of data taken with the prototype counters using a cosmic ray test stand will be presented and compared with a Monte Carlo simulation. We will also describe the algorithm for identifying single $p\bar{p}$ interaction events.

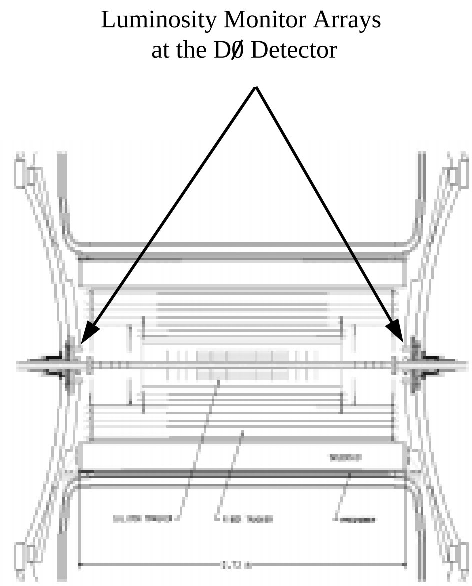

Figure 1. Side view of the Luminosity Monitor at the DØ Detector.

2. Counter Design

The DØ Run II Luminosity Monitor comprises two arrays of scintillation counters located on the inside faces of the end-cap calorimeters, 135 cm from the center of the DØ detector along the z direction (beam axis), and arranged symmetrically about the beam pipe. The detector covers a region in pseudorapidity of $2.7 < |\eta| < 4.4$, providing an acceptance of $(98 \pm 1)\%$ for detecting non-diffractive inelastic collisions (estimated from Monte Carlo studies). The location of the Luminosity Monitor counters on the DØ detector is shown in Fig. 1.

Each of the Luminosity Monitor arrays consists of 24 identical $5/8''$ thick BC-408 scintillator wedges, with Hamamatsu $1''$ diameter fine-mesh photomultiplier tubes (R5505) mounted directly on the faces. The layout of the counters is shown in Fig. 2. Advantages of the wedge design with the unconventional placement of the photomultiplier tubes include:

- Providing uniform counter occupancy that should improve multiple interaction detection and minimize photomultiplier aging,
- Aligning the tube axis with the magnetic field, as required for fine-mesh photomultiplier tubes,
- Providing good TOF resolution with a single photomultiplier tube, and
- Minimizing mechanical interference with other detector components and meeting the tight space constraints.

The counters will be located in a region where the magnetic field maps indicate a nearly axial magnetic field of ~ 1 Tesla. The fine-mesh photomultipliers are chosen to replace the conventional photomultipliers in order to be able to operate with high gain in large magnetic fields while maintaining the desirable low noise, fast risetime and good quantum efficiency of a photomultiplier tube. We tested two $1''$ diameter Hamamatsu fine-mesh photomultipliers in the DØ test beam facility. The tubes were oriented axial with the

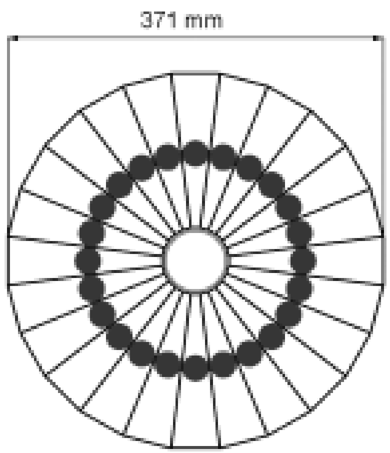

Figure 2. Schematic drawing of the Luminosity Monitor design with photomultipliers mounted of the face of wedge-shaped scintillators.

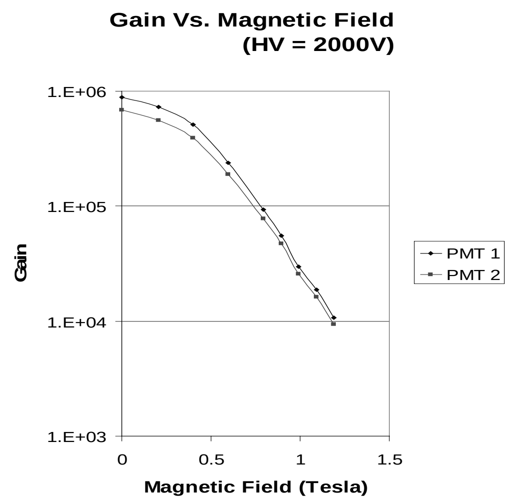

Figure 3. Gain versus magnetic field for two 1″ diameter fine-mesh photomultiplier tubes.

test beam magnetic field as in the DØ detector. The relative gain as a function of magnetic field is shown in Fig. 3 and is in good agreement with Hamamatsu specifications. A gain of $> 10{,}000$ @ 1 Tesla is sufficient for the Luminosity Monitor operation.

The measured arrival time of a charged particle depends on where the particle hits the counter, with hits near the photomultiplier appearing to be earlier than hits far from the tube. Since the position of the hit is unknown, the timing resolution is degraded. Figure 4 shows a Monte Carlo study of photon propagation times for charged particles hitting the counter close to the small radius end of the counter. The arrival time distribution (dashed line) has two peaks, which degrade the time resolution. The later peak corresponds to photons that propagate the length of the counter, reflect off the large radius end, and then propagate to the photomultiplier. This second peak is eliminated by putting an absorber on the large radius end of the counter as shown (solid line). Each counter will then be wrapped with aluminum foil.

3. Prototype Counter Tests

We have built prototypes of the Luminosity Monitor counters and measured their properties in a cosmic ray test stand. The test stand consists of two TOF reference counters and associated electronics. The test stand has a time resolution of 56 ps for predicting the arrival time of a particle striking the prototype counters, and a $\sim$ 1 cm precision on predicting the position of the particle hit.

The time resolution of a prototype Luminosity Monitor wedge counter can be obtained by comparing the recorded cosmic ray arrival time from the prototype counter with the predicted arrival time from the reference counters. Figure 5 shows a time resolution of 194 ps is achieved for a typical prototype counter after correcting for the test stand resolution.

The time resolution expected for the prototype counter depends on the intrinsic time resolution of the counter and the contribution to the resolution from the position dependence of the charged particle hit. The intrinsic time resolution of a scintillation counter typically scales as $n_{pe}^{-1/2}$ where n_{pe} is the number of photoelectrons

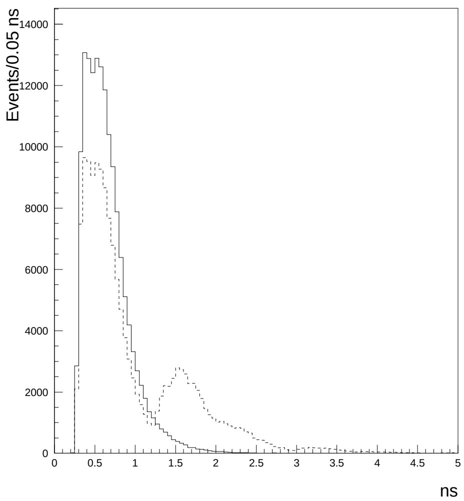

Figure 4. Photon propagation time for photons generated near the small radius end of the counter with absorber (solid line) or reflector (dashed line) placed at the large radius end. (The distributions are normalized to equal area.)

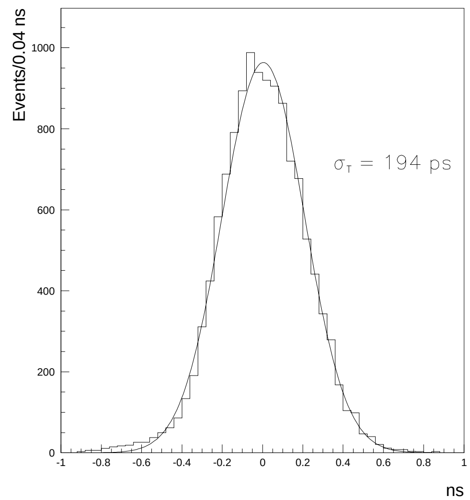

Figure 5. Difference between the measured and the predicted arrival times showing the resolution for a prototype Luminosity Monitor counter.

collected by the photomultiplier tube and is directly related to the photon collection efficiency. The light collection efficiency is observed to have a strong position dependence. Figure 6 shows the number of photoelectrons as a function of position measured by the cosmic ray test stand. Using the expected values of particle energy loss in the plastic scintillator, the scintillator light output, and the photomultiplier tube quantum efficiency, we can predict the expected number of photoelectrons using our simulation program. The simulation results are also shown in Fig. 6 and good agreement between data and simulation are seen.

The difference between the predicted and measured times as a function of position is shown in Fig. 7. The prototype test results are overlaid with the predictions of the simulation program and also show a good agreement.

4. Multiple Interaction Trigger Flags

The on-line multiple interaction trigger flags for the new Luminosity Monitor design are optimized to have high efficiency for detecting single $p\bar{p}$ interaction events while rejecting as many multiple $p\bar{p}$ interaction events as possible. The associated electronics for the digitization and readout are also being redesigned since the Fermilab accelerator operation in Run II is expected to provide beams with a shorter bunch spacing of 396 and 132 ns rather than 3.5 μs in Run I. We evaluated several multiple interaction trigger algorithms using a DTUJET [6] Monte Carlo sample generated with the expected spread in the time and position of the $p\bar{p}$ interactions.

A luminous region of 25 cm length in z direction is used for the 396 ns bunch spacing operation. The 132 ns bunch spacing operation requires a crossing angle at the $p\bar{p}$ collision point and the length of the luminous region is therefore shorter than in the 396 ns bunch spacing operation. A luminous region of 11 cm is used for the 132 ns bunch spacing case. The beam bunch length is about 37 cm for both 132 ns and 396 ns bunch spacing.

The performance of the algorithm is presented using the trigger efficiency for the single $p\bar{p}$ interaction events, and the trigger "rejection factor"

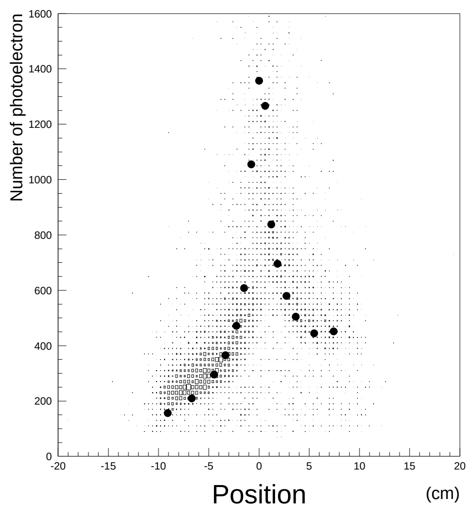

Figure 6. Number of photoelectrons versus charged particle hit position measured for a prototype counter (scatter plot) and the prediction from simulations (solid point). The origin of the position axis is underneath the photomultiplier with positive positions closer to the beam axis.

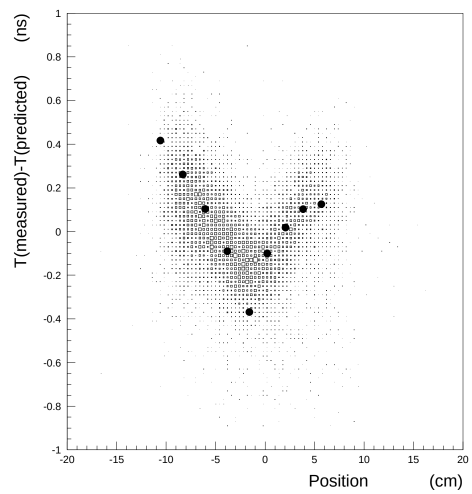

Figure 7. Difference between the measured and predicted arrival times versus charged particle hit position measured for a prototype counter (scatter plot) and the prediction from simulations (solid point). The origin of the position axis is underneath the photomultiplier with positive positions closer to the beam axis.

that is calculated as the ratio between the fraction of the single to double $p\bar{p}$ interaction events passing the algorithm. Figure 8 shows an algorithm that uses the time difference between the earliest and the third latest hits to distinguish between the single and double $p\bar{p}$ interactions in a beam crossing. We are able to retain 90% of the single interaction events with a rejection factor of 12 in the 396 bunch spacing operation, and a rejection factor of 7 in the 132 bunch spacing operation. The third latest hit is used in the algorithm to prevent single interaction events with a small number of out-of-time hits from being misidentified as multiple interactions.

5. Conclusion

The DØ Run II Luminosity Monitor consists of plastic scintillation detectors with fine-mesh photomultiplier readout. It is expected to provide a precise measurement of the rate for non-diffractive inelastic collisions, which will be used to calculate the Tevatron luminosity at DØ. The good time-of-flight resolution will allow an accurate measurement for the primary vertex position in the single $p\bar{p}$ interaction events as well as identification of the multiple interaction events. All aspects of the Run II Luminosity Monitor are well underway and scheduled to be complete by the spring of the year 2000.

REFERENCES

1. J. Bantly *et al.*, IEEE Trans. on Nucl. Sci. **41**, 1274 (1994).
2. Fermilab Technical Memo. TM-1911, 1930, 1995, 2000.
3. N. Amos *et al.*, Phys. Lett. **B243**, 158 (1990).
4. F. Abe *et al.*, Phys. Rev. D. **50**, 5518 (1994); F. Abe *et al.*, Phys. Rev. D. **50**, 5535 (1994); F. Abe *et al.*, Phys. Rev. D. **50**, 5550 (1994).
5. M. Tartaglia, FERMILAB-CONF-97-184-E.
6. P. Aurenche *et al.*, Phys. Rev. D. **45**, 92 (1992). See also, F.W. Bopp *et al.*, Z. Phys.

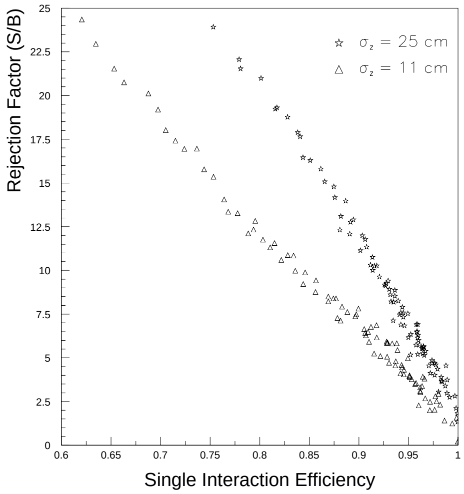

Figure 8. The single interaction trigger efficiency versus rejection factor for the algorithm using the difference between arrival times of the earliest and the third latest hits.

C51, 99 (1991).